



Published in final edited form as:

*J Pathol.* 2023 May ; 260(1): 97–107. doi:10.1002/path.6068.

## Liver Insulin-like Growth Factor-1 mediates effects of low-intensity vibration on wound healing in diabetic mice

Rita E. Roberts<sup>1,2,4</sup>, Jacqueline Cavalcante-Silva<sup>1,2,4</sup>, Mercedes Del Rio-Moreno<sup>3,4</sup>, Onur Bilgen<sup>5</sup>, Rhonda D. Kineman<sup>3,4</sup>, Timothy J. Koh<sup>1,2,4,\*</sup>

<sup>1</sup>Department of Kinesiology and Nutrition, University of Illinois at Chicago, Chicago, IL, USA

<sup>2</sup>Center for Tissue Repair and Regeneration, University of Illinois at Chicago, Chicago, IL, USA

<sup>3</sup>Department of Medicine, Section of Endocrinology, Diabetes and Metabolism, University of Illinois at Chicago, Chicago, IL, USA

<sup>4</sup>Jesse Brown VA Medical Center, Chicago, IL, USA

<sup>5</sup>Department of Mechanical & Aerospace Engineering, Rutgers University, Piscataway, NJ, USA

### Abstract

Chronic wounds in diabetic patients are associated with significant morbidity and mortality; however, few therapies are available to improve healing of diabetic wounds. Our group previously reported that low-intensity vibration (LIV) can improve angiogenesis and wound healing in diabetic mice. The purpose of the current study was to begin to elucidate mechanisms underlying LIV-enhanced healing. We first demonstrate that LIV-enhanced wound healing in db/db mice is associated with increased IGF1 protein levels in liver, blood, and wounds. The increase in IGF1 protein in wounds is associated with increased *Igf1* mRNA expression both in liver and wounds but the increase in protein levels preceded the increase in mRNA expression in wounds. Since our previous study demonstrated that liver is a primary source of IGF1 in skin wounds, we used inducible ablation of IGF1 in liver of high fat diet-fed (HFD) mice to determine whether liver IGF1 mediates the effects of LIV on wound healing. We demonstrate that knockdown of IGF1 in liver blunts LIV-induced improvements in wound healing in HFD mice, particularly increased angiogenesis and granulation tissue formation, and inhibits the resolution of inflammation. These studies indicate that LIV may promote skin wound healing at least in part via crosstalk between the liver and wound.

\*Correspondence to: TJ Koh, Department of Kinesiology and Nutrition, University of Illinois at Chicago, 1919 W. Taylor St. (m/c 994, Rm 650), Chicago, IL 60612, USA. tjkoh@uic.edu.

Author contributions statement

RR helped design the study, conducted experiments, performed assays, analyzed data and wrote the manuscript. JS and MD helped perform assays, analyze data, and write the manuscript. OB, RK and TK helped design the study, write the manuscript, and provided materials.

TK has a patent pending on the application of vibration for therapeutic treatment for tissue repair “Method and system for physical stimulation of tissue” (#2013/0165,824). No other conflicts of interest were declared

## Keywords

skin wound healing; impaired wound healing; chronic wound; diabetes complications; insulin-like growth factors; mechanical therapy; vibration therapy; skin-liver axis

---

## INTRODUCTION

Chronic wounds associated with diabetes are an ever-increasing health problem, with annual Medicare costs in the United States as high as \$13 billion [1,2]. People with diabetes incur a 25% lifetime risk of developing chronic wounds, which often lead to amputation, resulting in decreased quality of life, high morbidity and mortality [3-5]. Wound healing requires coordinated responses of diverse cell types over the course of healing and chronic wounds exhibit defects in each phase of healing, including dysregulated inflammation, impaired perfusion and neovascularization, and poor tissue formation and maturation [6,7]. However, few therapies are available to improve healing of diabetic wounds.

Energy-based treatment modalities, including laser, electrical, or mechanical stimulation are often used in conjunction with standard treatments for hard to heal chronic wounds [8,9]. Our group demonstrated that whole body low-intensity vibration (LIV) can improve angiogenesis and wound healing in diabetic mice, potentially by increasing growth factors such as insulin-like growth factor (IGF)-1 and vascular endothelial growth factor (VEGF) in the wound [10,11]. In addition, we and others have demonstrated that LIV increases skin blood flow [12-15] and can inhibit progression of pressure ulcers [16,17]. However, much remains to be learned about the mechanisms by which LIV signals influence wound healing.

Our previous studies showed that IGF1 is consistently increased in wounds of diabetic mice treated with LIV [10,11]. Wound IGF1 levels are reduced in diabetic mice and humans, which may contribute to impaired healing [6,18,19] and efforts to increase IGF1 levels in wounds of diabetic mice have produced positive effects on healing [20-23]. Importantly, IGF1 is present at high levels in the circulation and the liver is the major source of circulating IGF1 in mice [24]. We recently reported that the liver is a primary source of IGF1 in skin wounds of lean, healthy mice, and contributes to angiogenesis, granulation tissue formation and re-epithelialization [25]. In humans, IGF1 levels in wounds are correlated with those in blood, suggesting that blood is the primary source of wound IGF1 [26]. However, IGF1 is also produced by keratinocytes, fibroblasts and macrophages in skin wounds [18,27,28]. Thus, the impact of LIV on liver-derived or local wound-produced IGF1 remains to be determined as does the impact of LIV-induced IGF1 on wound healing.

In this study, we first demonstrated that LIV-enhanced wound healing is associated with increased IGF1 levels in liver and blood of diabetic db/db mice. We then demonstrated that knockdown of IGF1 in the liver blunted LIV-induced improvements in wound healing of high fat diet (HFD)-fed C57Bl/6 mice, a model of insulin resistance (pre-diabetes). These studies begin to elucidate the mechanisms by which LIV improves wound healing in mice and set the stage for translational studies in humans.

## Materials and methods

### Animals.

All animal studies were approved by the Animal Care and Use Committee of the Jesse Brown VA Medical Center. Diabetic db/db mice (BKS.Cg-Dock7m  $+/+$  Leprdb/J) and B6.129(FVB)-Igf1tm1Dlr/J mice were purchased from The Jackson Laboratory (Bar Harbor, ME, USA). The latter mice have loxP sites flanking exon 4 of the *Igf1* gene (*Igf1* fl/fl mice) to allow for Cre-mediated excision. Mice were housed in environmentally controlled conditions with a 12-h light/dark cycle. Water and food were available ad libitum. Each experiment was performed at least twice with a total of four male mice per group/condition. To minimize bias, mice were randomly assigned to experimental groups and resulting samples were coded and analyzed in a blinded fashion.

### High fat diet.

*Igf1* fl/fl mice were bred at the Jesse Brown VA Medical Center and were fed a high fat diet (HFD, 60 kcal%, Research Diets, New Brunswick, NJ, USA) for 16 weeks, starting when mice were weaned at 3–4 weeks old, to induce obesity and insulin resistance. Age-matched controls were fed normal diet (ND) over the same period.

### Blood glucose levels.

At entry into experimentation, db/db mice were ~12 weeks of age and *Igf1* fl/fl mice were ~20 weeks of age. For all mice, blood glucose levels were assessed via tail nick after a 4 h fast prior to experimentation and at time of euthanasia; db/db mice were only used if blood glucose was greater than 250 mg/dl.

### IGF1 ablation.

To ablate IGF1 specifically in liver hepatocytes, AAV8.pTBG.Cre (AAV-Cre) was injected via an retroorbital vein plexus in *Igf1* fl/fl mice to induce Cre-mediated recombination, and AAV8.pTBG.Null (AAV-Null) was injected for controls (Penn Vector Core, University of Pennsylvania, Philadelphia, PA, USA). AAV-Cre or AAV-Null was injected 7 days prior to wounding. AAV8-pTBG-Cre mediated recombination has proven to be highly specific for hepatocytes and induces greater than 90% reduction in the expression of the floxed allele for up to 8 months [25,29-31].

### Excisional wounding.

Mice were subjected to excisional wounding as described previously [10,11,25]. In brief, mice were anesthetized with isoflurane and their dorsum was shaved and cleaned with alcohol. Four 8 mm wounds were made on the back of each mouse with a dermal biopsy punch and covered with Tegaderm (3M, Minneapolis, MN, USA) to keep the wounds moist and maintain consistency with treatment of human wounds.

### Low-intensity vibration.

Mice were randomly assigned to whole-body LIV treatment or to a non-vibration sham (control) group. LIV treatment utilized low intensity signals (0.3 x *g* peak accelerations

delivered at 45 Hz) found to be effective in a previous study [11]. Harmonic LIV signals were calibrated using an accelerometer attached directly to top surface of the vibrating plate. For LIV treatment, mice were placed in an empty cage directly on a vibrating plate, and LIV was applied for 30 min per day for 7 days/week starting on the day of wounding. Non-vibrated sham controls were similarly placed in a separate empty cage but were not subjected to LIV.

### **Wound closure.**

Wound closure was assessed in digital images of the external wound surface taken immediately after injury and on days 3, 6 and 10 post-injury for db/db mice and on day 6 post-injury for HFD mice. Wound area was measured using Fiji ImageJ software (<https://imagej.net/software/fiji/>; downloaded 10/29/20) and expressed as a percentage of the area immediately after injury.

### **Wound histology.**

Re-epithelialization and granulation tissue thickness were measured in cryosections taken from the center of the wound (found by serial sectioning through the entire wound) and stained with hematoxylin and eosin [19,25,32]. Digital images were obtained using a Keyence BZ-X710 All-in-One Fluorescence Microscope (Keyence, Itasca, IL, USA) with a 2x or 20x objective and analyzed using ImageJ software. The percentage of re-epithelialization, length of epithelial tongues and granulation tissue area were measured in three sections per wound and was averaged over sections to provide a representative value for each wound.

Angiogenesis was assessed by immunohistochemical staining for CD31 (390, 1:100; BioLegend, San Diego, CA, USA), macrophage accumulation by staining for F4/80 (BM8, 1:100, Thermo Fisher, Waltham, MA, USA) and neutrophil accumulation by staining for Ly6G (1A8, 1:100, BD Pharmingen, Franklin Lakes, NJ, USA). Collagen deposition was assessed using Masson trichrome staining (IMEB, San Marcos, CA, USA). For each assay, digital images were obtained covering the wound bed (2 or 3 fields using a 20x objective) and the percent area stained was quantified by the number of clearly stained pixels above a threshold intensity and normalizing to the total number of pixels. The software allowed the observer to exclude artifacts. For each assay, three sections per wound were analyzed.

### **ELISA.**

Liver or wound samples were homogenized in ice-cold Tris (40 mM) buffer (supplemented with 1 mM EDTA, 5 mM EGTA, 25 mM  $\beta$ -glycerophosphate, 25 mM NaF, 1 mM  $\text{Na}_3\text{VO}_4$ , and a protease inhibitor cocktail (Millipore Sigma, Burlington, MA, USA); 10  $\mu\text{l}$  per mg liver or wound tissue) using a Dounce homogenizer and then centrifuged and supernatant collected. Blood was collected by retroorbital bleed into EDTA tubes, and then centrifuged to obtain plasma. Samples were used for Igf1, I11b (R&D Systems, Minneapolis, MN, USA), growth hormone (Merck, Rahway, NJ, USA) and insulin (Merckodia, Winston-Salem, NC, USA) ELISAs following the manufacturers' instructions. All samples were run in duplicate, and all important comparisons were run on the same plate.

## RT-qPCR.

Tissue samples were homogenized using Trizol reagent (Thermo Fisher) and a bead homogenizer. Homogenates were centrifuged and supernatants were used for RNA isolation. RNA concentration was measured using a Nanodrop 2000 spectrophotometer (Thermo Fisher) and equal amounts of RNA were reverse transcribed using a High Capacity cDNA Reverse Transcription Kit (Thermo Fisher). mRNA expression levels were assessed using Power SYBR Green PCR Master Mix (Thermo Fisher) and the ViiA7 Real-Time PCR System (Thermo Fisher). The copy numbers of all mRNA transcripts in tissue homogenates were adjusted following calculation of individual normalization factors for *Gapdh* and *Rpl4* reference genes using GeNorm 3.3, as described previously [33]. Primers sequences used: *Gapdh* (F: 5'- ATGGCCTTCCGTGTTCCCTAC-3' / R: 5'- CCTGCTTCACCACCTTCTT), *Rpl4* (F: 5'-GGATGTTGCGGAAGGCCTTGA-3' / R: 5'-GAGCTGGCAAGGGCAAATGAG-3') and *Igf1* (F: 5'- ACAGGCTATGGCTCCAGCA-3' / R: 5'-GCACAGTACATCTCCAGTCTCCTC-3').

## Statistics.

Data are expressed as mean  $\pm$  SD. Statistical significance of differences was evaluated by two-way ANOVA models. For experiments with db/db mice, the model tested for effects of LIV treatment (2 levels: sham and LIV) and time (3 levels: days 3, 6, and 10 days) and LIV treatment-by-time interaction effects. For experiments with HFD mice, the model tested for effects of LIV treatment (2 levels: sham and LIV) and liver IGF1 knockdown (2 levels: AAV-Null and AAV-Cre) and LIV treatment-by-liver IGF1 knockdown effects. Šidák's multiple comparison *post hoc* test was used to assess differences between LIV treatment groups at each time point or in each IGF1 knockdown group.  $P < 0.05$  was considered statistically significant.

## RESULTS

### LIV promotes wound healing in diabetic db/db mice.

Our previous studies have shown that whole-body LIV applied at 45 Hz frequency and 0.3–0.4 g acceleration increases angiogenesis and granulation tissue formation and accelerates wound closure in diabetic db/db mice [10,11]. However, these studies focused on later stages of healing (7 days post-injury and later); in the present study we assessed effects starting on day 3 post-injury. First, we confirmed that LIV improved both epidermal and dermal wound healing (Figure 1A-D). LIV accelerated wound closure, assessed both by external measurements of wound area made in digital images of the wound surface (Figure 1E) and by histological measurements of re-epithelialization and epithelial tongue lengths (Figure 1F,G). For each measurement of wound closure, LIV showed little effect on day 3, but had significant effects on days 6 and 10 post-injury. Next, we assessed the effect of LIV on granulation tissue formation and dermal healing. Again, LIV showed little effect on granulation tissue area and angiogenesis (CD31 staining) on day 3, but had significant effects on days 6 and 10 post-injury (Figure 1H,I). In contrast, there were no significant effects of LIV on collagen deposition at any time point, as assessed by Trichrome staining (Figure 1J). Also, there were no significant effects of LIV on either body weight or blood

glucose levels at any of the time points examined (Table 1), thereby excluding these variables as potential contributors to improved wound healing in LIV-treated mice.

To begin to elucidate the mechanism underlying improved wound healing induced by LIV, we assessed effects of LIV on IGF1 protein and *Igf1* mRNA expression; we found that LIV increased IGF1 protein levels in wounds starting on day 3 post-injury (Figure 2A) but only increased *Igf1* mRNA expression on day 6 (Figure 2D). Because of the discordance of the time course in wound *Igf1* mRNA and protein, and our previous study indicating that liver is a primary source of IGF1 that accumulates in wounds, we also measured IGF1 levels in blood and liver. Interestingly, LIV increased IGF1 protein levels in blood on days 3 and 6 post-injury and in liver on days 6 and 10 (Figure 2B,C). In addition, LIV increased *Igf1* mRNA in liver on day 3 post-injury (Figure 2E). These findings indicated a systemic effect of LIV on IGF1 production and indicate that the liver may be a source of the increased wound IGF1 levels observed with LIV treatment.

### **Liver IGF1 knockdown reduces wound IGF1 levels in obese and insulin resistant HFD mice and prevents LIV-induced increases in IGF1.**

To determine whether liver IGF1 mediates the effects of LIV on wound healing, we used floxed *Igf1* mice that allowed inducible knockdown of liver IGF1 following injection with AAV8-pTBG-Cre [25,29-31]. We fed floxed *Igf1* mice either ND or HFD for 4 months, the latter to induce a pre-diabetic state, then subjected each group to excisional wounding and either LIV or sham control treatment. As expected, HFD fed mice showed significantly increased body weight and insulin levels compared to ND fed mice (Table 2 and supplementary material, Table S1). Also as expected, two-way ANOVA analysis of liver IGF1 protein levels indicated a significant main effect of liver IGF1 knockdown ( $P<0.001$ ) and there was a significant interaction between liver IGF1 knockdown and LIV treatment ( $p=0.02$ ). *Post hoc* analysis indicated that LIV treatment tended to increase liver IGF1 protein levels in AAV-null treated mice ( $p=0.06$ ; Figure 3A). In addition, AAV-Cre treated mice exhibited near complete ablation of IGF1 in liver, and LIV did not alter in liver IGF1 levels in these mice. For blood IGF1 levels, two-way ANOVA analysis only showed a significant main effect of liver IGF1 knockdown ( $P<0.001$ ; Figure 3B). For wound IGF1 levels, two-way ANOVA analysis indicated a significant main effect of liver IGF1 knockdown ( $P<0.001$ ) and there was a trend of an effect of LIV treatment ( $p=0.053$ ). Similar to our previous study of ND fed mice [25], liver IGF1 knockdown reduced wound IGF1 levels by ~50% in HFD mice. *Post hoc* analysis indicated a trend of an increase in IGF1 levels with LIV treatment in AAV-Null ( $p=0.07$ ) but not AAV-Cre treated mice (Figure 3C). When assessing *Igf1* mRNA levels, liver showed only a significant effect of liver IGF1 knockdown (Figure 3D) and wounds showed no significant effects of either liver IGF1 knockdown or LIV treatment (Figure 3E).

In parallel studies of ND-fed mice, we found no effect of LIV on IGF1 levels in liver, plasma, or wounds in either control mice or in IGF1 knockdown mice (supplementary material, Figure S1). In addition, there were no significant differences in either body weight, blood glucose or growth hormone levels between sham-treated and LIV-treated groups, either before or after wounding, in either ND-fed (supplementary material, Table S1) or

HFD-fed mice (Table 2), excluding these variables as contributors to effects of LIV on wound healing. There was a significant increase in growth hormone levels in AAV-Cre treated animals compared to AAV-Null treated animals, in both ND-fed and HFD-fed mice, due to lack of feedback inhibition of circulating IGF1 on growth hormone production [34], but there was no significant effect of LIV on growth hormone levels in either ND or HFD mice. In summary, liver IGF1 may account for the trends of increased wound IGF1 levels induced by LIV treatment in HFD mice.

#### **LIV may accelerate wound closure in HFD mice in a liver IGF1-dependent manner.**

LIV induced a trend of improved epidermal healing and significantly improved dermal healing in AAV-Null treated mice but not in AAV-Cre treated mice (Figure 4A-H). Two-way ANOVA analysis indicated significant main effects of both LIV ( $p=0.02$ ) and liver IGF1 knockdown ( $P<0.001$ ) on external measurements of wound closure, and *post hoc* analysis indicated that LIV induced a trend of an increase in control mice ( $p=0.07$ ) but not in mice with liver IGF1 knockdown (Figure 4I). Histological measurements of re-epithelialization showed similar results, as two-way ANOVA analysis indicated a significant main effect of liver IGF1 knockdown ( $p=0.02$ ), and *post hoc* analysis indicated that LIV induced a trend of an increase in control mice ( $p=0.10$ ) but not in mice with liver IGF1 knockdown (Figure 4J). In parallel studies of ND-fed mice, we found no effect of LIV on wound closure or re-epithelialization in either control mice or in IGF1 knockdown mice (supplementary material, Figure S1).

#### **LIV increases granulation tissue formation and angiogenesis in HFD mice in an liver IGF1-dependent manner.**

Two-way ANOVA analysis indicated significant main effects of both LIV ( $p=0.02$ ) and liver IGF1 knockdown ( $p=0.006$ ) on histological measurement of granulation tissue area, and *post hoc* analysis indicated that LIV induced a significant increase in control mice ( $p=0.01$ ) but not in mice with liver IGF1 knockdown (Figure 4K). Assessment of angiogenesis using immunohistochemical staining for CD31 showed similar results, as two-way ANOVA analysis indicated significant main effects of both LIV ( $p=0.03$ ) and liver IGF1 knockdown ( $p=0.008$ ), and *post hoc* analysis indicated that LIV induced a significant increase in control mice ( $p=0.04$ ) but not in mice with liver IGF1 knockdown (Figure 4L). In contrast, LIV treatment did not have an effect on collagen deposition as assessed by Trichrome staining in either AAV-Null treated or AAV-Cre treated groups (Figure 4M). In parallel studies of ND-fed mice, we found no effect of LIV on granulation tissue area or angiogenesis in either control mice or in IGF1 knockdown mice (supplementary material, Figure S1).

#### **LIV reduces neutrophil accumulation and wound IL-1 $\beta$ expression in HFD mice in a liver IGF1-dependent manner.**

Two-way ANOVA analysis indicated significant main effects of both LIV ( $p=0.004$ ) and liver IGF1 knockdown ( $p=0.03$ ) on histological measurements of Ly6G<sup>+</sup> neutrophil accumulation, and *post hoc* analysis indicated that LIV induced a significant decrease in control mice ( $p=0.004$ ) but not in mice with liver IGF1 knockdown (Figure 5A-E). In contrast, neither LIV nor liver IGF1 knockdown had an effect on F4/80<sup>+</sup> macrophage accumulation (Figure 5F). In addition, two-way ANOVA analysis showed significant main

effects of both LIV ( $p=0.05$ ) and liver IGF1 knockdown ( $p=0.03$ ) on levels of IL-1 $\beta$  in wounds and there was a significant interaction effect between LIV treatment and liver IGF1 knockdown ( $p=0.01$ ). *Post hoc* analysis indicated that LIV induced a significant decrease in control mice ( $p=0.004$ ) but not in mice with liver IGF1 knockdown (Figure 5G). Finally, in parallel studies of ND-fed mice, we found no effect of LIV on neutrophil or macrophage accumulation, or in levels of IL-1 $\beta$  levels, in either control mice or in IGF1 knockdown mice (supplementary material, Figure S1).

## DISCUSSION

Despite the escalating socioeconomic impact of diabetic wounds, effective treatments remain elusive. Our group previously reported that application of LIV can improve wound healing in diabetic mice [10,11]. Here, we begin to elucidate mechanisms mediating this LIV-enhanced healing. We first demonstrate that whole body LIV increases IGF1 protein levels in liver, blood, and wounds in db/db mice. The increase in IGF1 protein in wounds was associated with increased *Igf1* mRNA expression both in liver and wounds but the increase in protein levels preceded the increase in mRNA expression in wounds. Since our previous study demonstrated that liver is a primary source of IGF1 in skin wounds [25], we used inducible ablation of IGF1 in liver of HFD mice to determine whether liver IGF1 mediates the effects of LIV on wound healing. We found that knockdown of IGF1 in liver blunts LIV-induced improvements in wound healing in HFD mice, particularly the increased angiogenesis and granulation tissue formation, and inhibits the resolution of inflammation. Thus, liver IGF1 appears to at least partly mediate the effect of LIV on skin wound healing.

The results of the current study are consistent with our previous studies, in which we reported that LIV delivered at 45 Hz and 0.2–0.3 x *g*, increased angiogenesis, granulation tissue formation, and re-epithelialization in diabetic mice [10,11]. Interestingly, our previous study also showed that LIV signals with higher frequency and/or greater acceleration do not positively influence skin wound healing [11]. This is paralleled by findings from a previous study on negative pressure therapy, for which protocols that induced rapid changes in pressure was detrimental to granulation tissue formation [35]. Other studies have demonstrated that LIV with similar frequency (47 Hz) and acceleration (0.2 x *g*) improves healing of stage I pressure ulcers in elderly patients compared to standard care [16] and reduced progression of pressure-induced deep tissue injury in rats – associated with downregulation of matrix metalloproteinase-2 and -9 activity [17]. Finally, a range of LIV signals have been shown to acutely increase skin blood flow, perhaps in a nitric oxide-dependent manner [12,36-38]. These latter studies highlight additional mechanisms by which LIV can improve wound healing, apart from the IGF1 mechanism observed in the present study.

We also reported previously that LIV increases IGF1 levels in wounds of diabetic mice [10,11]. In the current study, the effects of LIV on IGF1 levels in wounds of HFD mice were less pronounced than in db/db mice, and were non-existent in lean, non-diabetic mice. These findings correlated with effects on wound healing as LIV had strong effects on angiogenesis, granulation, and wound closure in db/db mice, more modest effects in HFD mice and no

effects in lean mice. Thus, LIV signals appear to have greatest effect in context for which healing is most impaired.

Although LIV produced only trends for increased wound closure and re-epithelialization of wounds in HFD mice, LIV significantly increased angiogenesis and granulation tissue. These data indicate that LIV may have stronger effects on dermal healing than on epidermal healing. Other mechanical energy-based modalities have also shown strong effects on dermal healing [8,9,39]. Consistent with our previous study in lean mice [25], knockdown of liver IGF1 reduced wound IGF1 levels in HFD mice. Importantly, LIV did not positively influence angiogenesis, granulation or wound closure when HFD mice were subjected to liver-specific IGF1 knockdown, indicating that liver IGF1 mediates at least some of the effects of LIV on wound healing. IGF1 likely promotes dermal and epidermal healing in wounds through its ability to promote proliferation and migration of multiple cell types including fibroblasts, endothelial cells and keratinocytes [21,22,40-43]. In addition, a number of studies have demonstrated that exogenous IGF1 can improve both dermal and epidermal healing in mice [20-23].

Finally, we found that LIV reduced neutrophil accumulation and IL-1 $\beta$  levels in HFD mice, indicating an anti-inflammatory effect. This anti-inflammatory effect of LIV again appeared to be liver IGF1 dependent. Interestingly, locally administered IGF1 reduced neutrophil accumulation in wounds of ovariectomized mice [21], consistent with the idea that IGF1 can play an anti-inflammatory role in wounds.

In summary, our findings demonstrated that LIV promotes wound healing in both diabetic db/db mice and pre-diabetic HFD mice. LIV-enhanced wound healing is associated with increased IGF1 levels in liver, blood and wounds, and knockdown of IGF1 in liver blocked the LIV-induced improvements in wound healing observed in HFD mice. These studies begin to elucidate the mechanisms by which LIV improves wound healing in mice and set the stage for translational studies in humans.

## Supplementary Material

Refer to Web version on PubMed Central for supplementary material.

## Acknowledgments

This study was supported by VA grant I01 RX002636 to RDK, OB and TJK, and NIGMS grant R35 GM136228 to TJK

## Data availability statement

Full data are available from the corresponding author upon reasonable request.

## REFERENCES

1. Magliano DJ, Islam RM, Barr ELM, et al. Trends in incidence of total or type 2 diabetes: systematic review. *BMJ* 2019; 366: 15003. [PubMed: 31511236]
2. Geraghty T, LaPorta G. Current health and economic burden of chronic diabetic osteomyelitis. *Expert Rev Pharmacoecon Outcomes Res* 2019; 19: 279–286. [PubMed: 30625012]

3. Hoffstad O, Mitra N, Walsh J, et al. Diabetes, lower-extremity amputation, and death. *Diabetes Care* 2015; 38: 1852–1857. [PubMed: 26203063]
4. Jeffcoate WJ, Harding KG. Diabetic foot ulcers. *Lancet* 2003; 361: 1545–1551. [PubMed: 12737879]
5. Ramsey SD, Newton K, Blough D, et al. Incidence, outcomes, and cost of foot ulcers in patients with diabetes. *Diabetes Care* 1999; 22: 382–387. [PubMed: 10097914]
6. Blakytyn R, Jude E. The molecular biology of chronic wounds and delayed healing in diabetes. *Diabet Med* 2006; 23: 594–608. [PubMed: 16759300]
7. Falanga V Wound healing and its impairment in the diabetic foot. *Lancet* 2005; 366: 1736–1743. [PubMed: 16291068]
8. Ennis WJ, Lee C, Gellada K, et al. Advanced Technologies to Improve Wound Healing: Electrical Stimulation, Vibration Therapy, and Ultrasound-What Is the Evidence? *Plast Reconstr Surg* 2016; 138: 94S–104S. [PubMed: 27556780]
9. Glass GE, Murphy GF, Esmaeili A, et al. Systematic review of molecular mechanism of action of negative-pressure wound therapy. *Br J Surg* 2014; 101: 1627–1636. [PubMed: 25294112]
10. Weinheimer-Haus EM, Judex S, Ennis WJ, et al. Low-intensity vibration improves angiogenesis and wound healing in diabetic mice. *PLoS One* 2014; 9: e91355. [PubMed: 24618702]
11. Roberts RE, Bilgen O, Kineman RD, et al. Parameter-Dependency of Low-Intensity Vibration for Wound Healing in Diabetic Mice. *Front Bioeng Biotechnol* 2021; 9: 654920. [PubMed: 33768089]
12. Tzen YT, Weinheimer-Haus EM, Corbiere TF, et al. Increased skin blood flow during low intensity vibration in human participants: Analysis of control mechanisms using short-time Fourier transform. *PLoS One* 2018; 13: e0200247. [PubMed: 30001409]
13. Nakagami G, Sanada H, Matsui N, et al. Effect of vibration on skin blood flow in an in vivo microcirculatory model. *Biosci Trends* 2007; 1: 161–166. [PubMed: 20103887]
14. Maloney-Hinds C, Petrofsky JS, Zimmerman G. The effect of 30 Hz vs. 50 Hz passive vibration and duration of vibration on skin blood flow in the arm. *Med Sci Monit* 2008; 14: CR112–116. [PubMed: 18301353]
15. Zhu T, Wang Y, Yang J, et al. Wavelet-based analysis of plantar skin blood flow response to different frequencies of local vibration. *Physiol Meas* 2020; 41: 025004. [PubMed: 31962305]
16. Arashi M, Sugama J, Sanada H, et al. Vibration therapy accelerates healing of Stage I pressure ulcers in older adult patients. *Adv Skin Wound Care* 2010; 23: 321–327. [PubMed: 20562541]
17. Sari Y, Sanada H, Minematsu T, et al. Vibration inhibits deterioration in rat deep-tissue injury through HIF1-MMP axis. *Wound Repair Regen* 2015; 23: 386–393. [PubMed: 25801385]
18. Brown DL, Kane CD, Chernausk SD, et al. Differential expression and localization of insulin-like growth factors I and II in cutaneous wounds of diabetic and nondiabetic mice. *Am J Pathol* 1997; 151: 715–724. [PubMed: 9284820]
19. Mirza RE, Fang MM, Ennis WJ, et al. Blocking interleukin-1beta induces a healing-associated wound macrophage phenotype and improves healing in type 2 diabetes. *Diabetes* 2013; 62: 2579–2587. [PubMed: 23493576]
20. Balaji S, LeSaint M, Bhattacharya SS, et al. Adenoviral-mediated gene transfer of insulin-like growth factor 1 enhances wound healing and induces angiogenesis. *J Surg Res* 2014; 190: 367–377. [PubMed: 24725678]
21. Emmerson E, Campbell L, Davies FC, et al. Insulin-like growth factor-1 promotes wound healing in estrogen-deprived mice: new insights into cutaneous IGF1R/ERalpha cross talk. *J Invest Dermatol* 2012; 132: 2838–2848. [PubMed: 22810305]
22. Semenova E, Koegel H, Hasse S, et al. Overexpression of mIGF1 in keratinocytes improves wound healing and accelerates hair follicle formation and cycling in mice. *Am J Pathol* 2008; 173: 1295–1310. [PubMed: 18832567]
23. Tsuboi R, Shi CM, Sato C, et al. Co-administration of insulin-like growth factor (IGF)-I and IGF-binding protein-1 stimulates wound healing in animal models. *J Invest Dermatol* 1995; 104: 199–203. [PubMed: 7530269]
24. Yakar S, Liu JL, Stannard B, et al. Normal growth and development in the absence of hepatic insulin-like growth factor I. *Proc Natl Acad Sci U S A* 1999; 96: 7324–7329. [PubMed: 10377413]

25. Roberts RE, Cavalcante-Silva J, Kineman RD, et al. Liver is a primary source of insulin-like growth factor-1 in skin wound healing. *J Endocrinol* 2021; 252: 59–70. [PubMed: 34708691]
26. Wagner S, Coerper S, Fricke J, et al. Comparison of inflammatory and systemic sources of growth factors in acute and chronic human wounds. *Wound Repair Regen* 2003; 11: 253–260. [PubMed: 12846912]
27. Gartner MH, Benson JD, Caldwell MD. Insulin-like growth factors I and II expression in the healing wound. *J Surg Res* 1992; 52: 389–394. [PubMed: 1350650]
28. Todorovic V, Pesko P, Micev M, et al. Insulin-like growth factor-I in wound healing of rat skin. *Regul Pept* 2008; 150: 7–13. [PubMed: 18597865]
29. Cordoba-Chacon J, Majumdar N, List EO, et al. Growth Hormone Inhibits Hepatic De Novo Lipogenesis in Adult Mice. *Diabetes* 2015; 64: 3093–3103. [PubMed: 26015548]
30. Wolf Greenstein A, Majumdar N, Yang P, et al. Hepatocyte-specific, PPARgamma-regulated mechanisms to promote steatosis in adult mice. *J Endocrinol* 2017; 232: 107–121. [PubMed: 27799461]
31. Sarmiento-Cabral A, Del Rio-Moreno M, Vazquez-Borrego MC, et al. GH directly inhibits steatosis and liver injury in a sex-dependent and IGF1-independent manner. *J Endocrinol* 2021; 248: 31–44. [PubMed: 33112796]
32. Mirza RE, Fang MM, Weinheimer-Haus EM, et al. Sustained inflammasome activity in macrophages impairs wound healing in type 2 diabetic humans and mice. *Diabetes* 2014; 63: 1103–1114. [PubMed: 24194505]
33. Vandesompele J, De Preter K, Pattyn F, et al. Accurate normalization of real-time quantitative RT-PCR data by geometric averaging of multiple internal control genes. *Genome Biol* 2002; 3: RESEARCH0034. [PubMed: 12184808]
34. Kineman RD, Del Rio-Moreno M, Sarmiento-Cabral A. 40 YEARS of IGF1: Understanding the tissue-specific roles of IGF1/IGF1R in regulating metabolism using the Cre/loxP system. *J Mol Endocrinol* 2018; 61: T187–T198. [PubMed: 29743295]
35. Dastouri P, Helm DL, Scherer SS, et al. Waveform modulation of negative-pressure wound therapy in the murine model. *Plast Reconstr Surg* 2011; 127: 1460–1466. [PubMed: 21460654]
36. Ichioka S, Yokogawa H, Nakagami G, et al. In vivo analysis of skin microcirculation and the role of nitric oxide during vibration. *Ostomy Wound Manage* 2011; 57: 40–47. [PubMed: 21918246]
37. Johnson PK, Feland JB, Johnson AW, et al. Effect of whole body vibration on skin blood flow and nitric oxide production. *J Diabetes Sci Technol* 2014; 8: 889–894. [PubMed: 24876449]
38. Maloney-Hinds C, Petrofsky JS, Zimmerman G, et al. The role of nitric oxide in skin blood flow increases due to vibration in healthy adults and adults with type 2 diabetes. *Diabetes Technol Ther* 2009; 11: 39–43. [PubMed: 19132854]
39. Vander Horst MA, Raeman CH, Dalecki D, et al. Time- and Dose-Dependent Effects of Pulsed Ultrasound on Dermal Repair in Diabetic Mice. *Ultrasound Med Biol* 2021; 47: 1054–1066. [PubMed: 33454160]
40. Brandt K, Grunler J, Brismar K, et al. Effects of IGFBP-1 and IGFBP-2 and their fragments on migration and IGF-induced proliferation of human dermal fibroblasts. *Growth Horm IGF Res* 2015; 25: 34–40. [PubMed: 25468444]
41. Deng M, Wang Y, Zhang B, et al. New proangiogenic activity on vascular endothelial cells for C-terminal mechano growth factor. *Acta Biochim Biophys Sin (Shanghai)* 2012; 44: 316–322. [PubMed: 22382131]
42. Kanekar S, Borg TK, Terracio L, et al. Modulation of heart fibroblast migration and collagen gel contraction by IGF-I. *Cell Adhes Commun* 2000; 7: 513–523. [PubMed: 11051461]
43. Nakao-Hayashi J, Ito H, Kanayasu T, et al. Stimulatory effects of insulin and insulin-like growth factor I on migration and tube formation by vascular endothelial cells. *Atherosclerosis* 1992; 92: 141–149. [PubMed: 1378740]

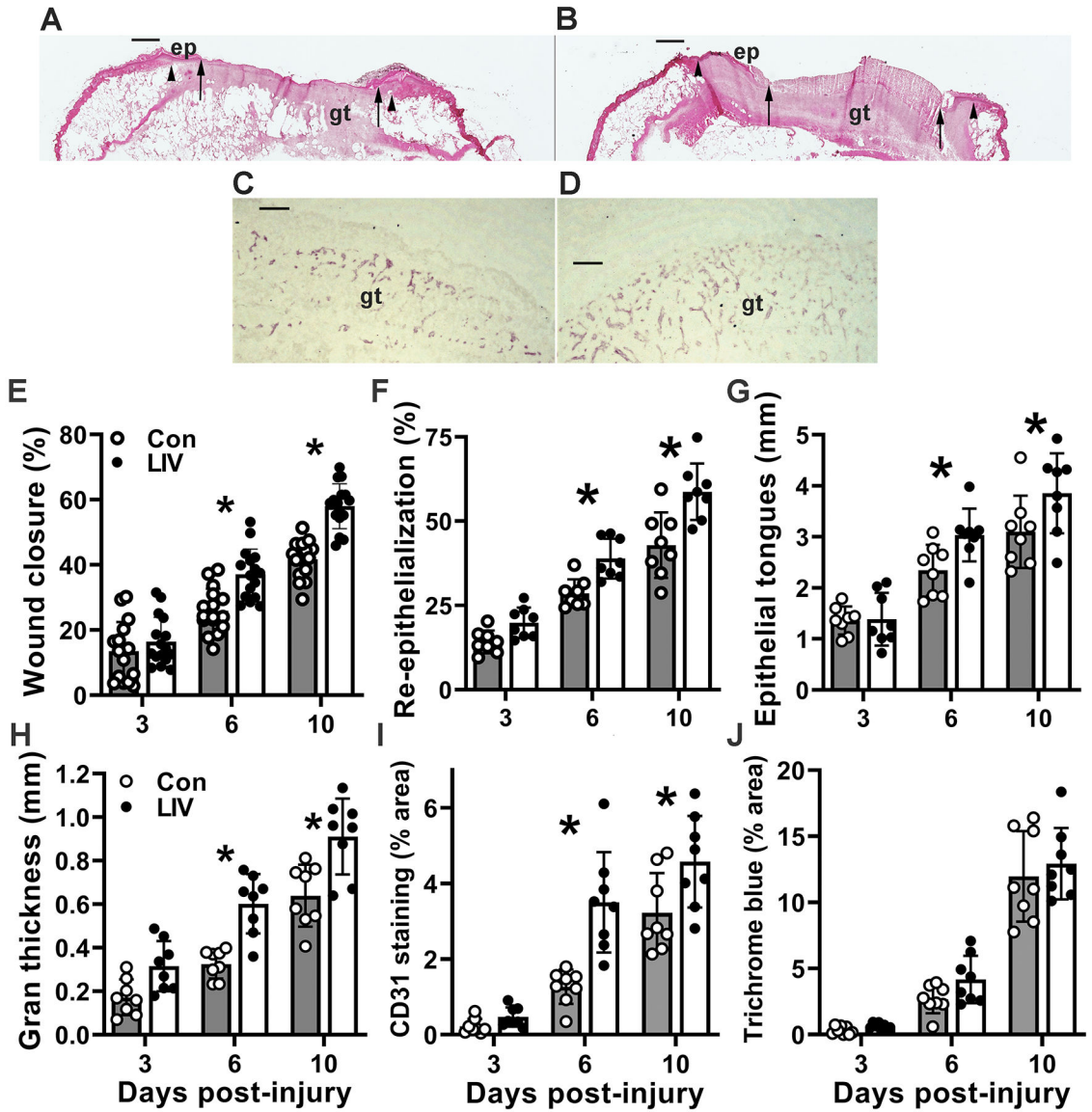


**Figure 1. LIV improves wound healing in diabetic mice.**

Diabetic db/db mice received whole-body LIV or sham control treatment (Con) for 30 min per day. Wound healing assessed on days 3, 6 and 10 post-injury. (A,B) Representative images of hematoxylin and eosin stained cryosections of center of day 10 wounds from sham-treated and LIV-treated db/db mice. ep: epithelium, gt: granulation tissue. Arrowheads indicate wound edges and arrows indicate tips of epithelial tongues migrating into wound. Scale bar, 0.5 mm. (C,D) Representative images of CD31 stained cryosections of the center of day 6 wounds from sham-treated and LIV-treated db/db mice. gt: granulation tissue. Scale bar, 100  $\mu$ m. (E) Wound closure assessed in digital images of wound surface, expressed as % closure from original wound area. (F) Re-epithelialization assessed in cryosections of wound center, expressed as % closure from wound edges in section. (G) Length of epithelial tongues measured in cryosections of wound center, measured as distance between wound edge to end of epithelial tongue, summed across the two sides of the wound. (H)

Granulation tissue area assessed in cryosections of wound center. (I) Angiogenesis assessed in cryosections of wound center expressed as % area stained for CD31. (J) Collagen deposition assessed in Trichrome stained cryosections of wound center, expressed as % area stained blue. For each data set except Trichrome staining, two-way ANOVA showed significant main effects of LIV treatment and time point. \* mean values significantly different between sham-treated and LIV-treated mice at indicated time point by Šidák's multiple comparisons test;  $P < 0.05$ . Mean  $\pm$  SD, n = 2–4 wounds from each of 4 mice per assay.

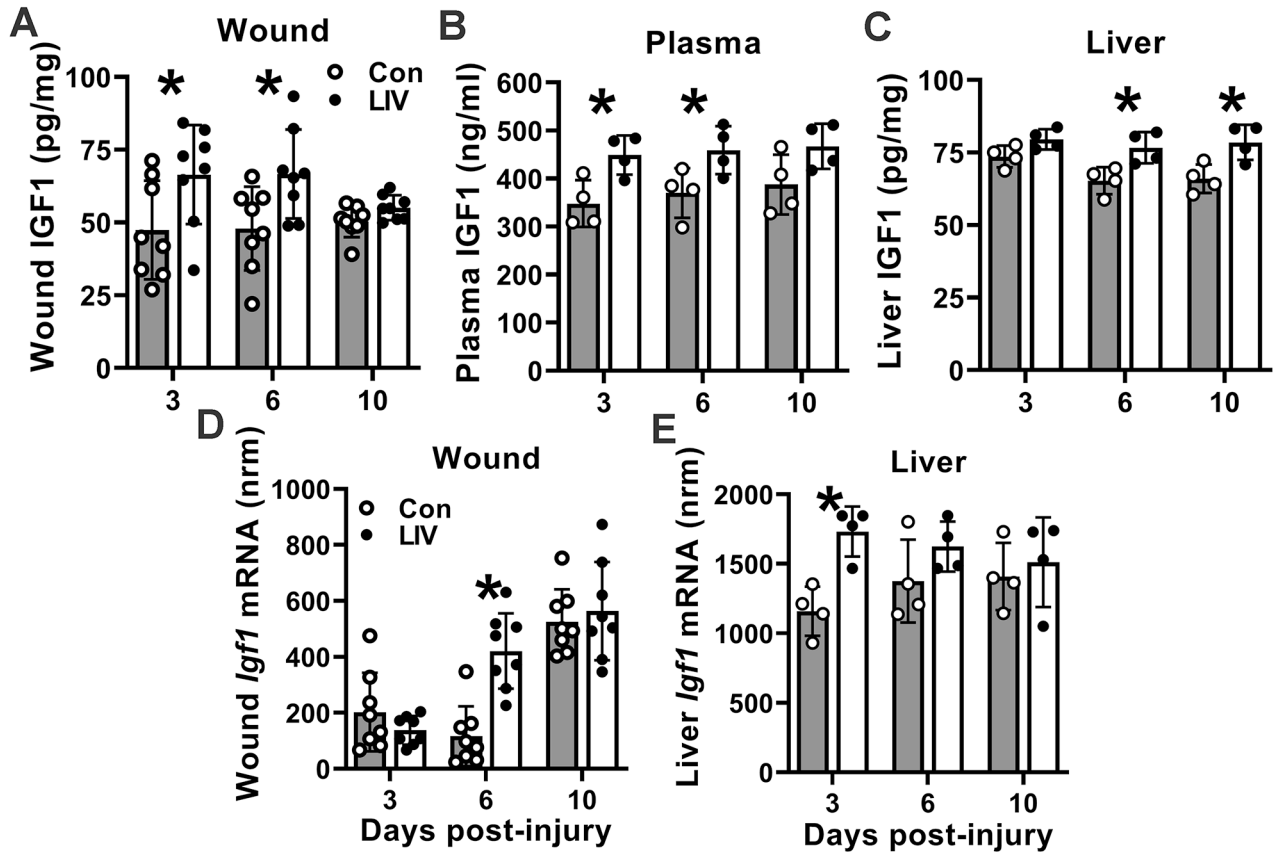


**Figure 2. LIV increases IGF1 levels in wounds, peripheral blood, and liver of diabetic mice.** Diabetic db/db mice received whole-body LIV or sham control treatment (Con) for 30 min per day. IGF1 levels assessed on days 3, 6 and 10 post-injury. (A–C) Wound, peripheral blood plasma, and liver IGF1 protein levels assessed by ELISA. (D,E) Wound and liver *Igf1* mRNA levels assessed by RT-qPCR. *Igf1* mRNA copy numbers normalized (nrm) to those of *Gapdh* and *Rpl4* reference transcripts. For each protein data set, two-way ANOVA showed significant main effects of LIV treatment. For wound mRNA data, two-way ANOVA showed significant main effects of LIV treatment and time point. For liver mRNA data, two-way ANOVA showed significant main effects of LIV treatment. \*mean values significantly different between sham-treated and LIV-treated mice at indicated time point by Šidák's multiple comparisons test;  $P < 0.05$ . Mean  $\pm$  SD. For wounds,  $n = 2$  wounds from each of 4 mice per assay. For plasma and liver,  $n = 4$  mice per assay

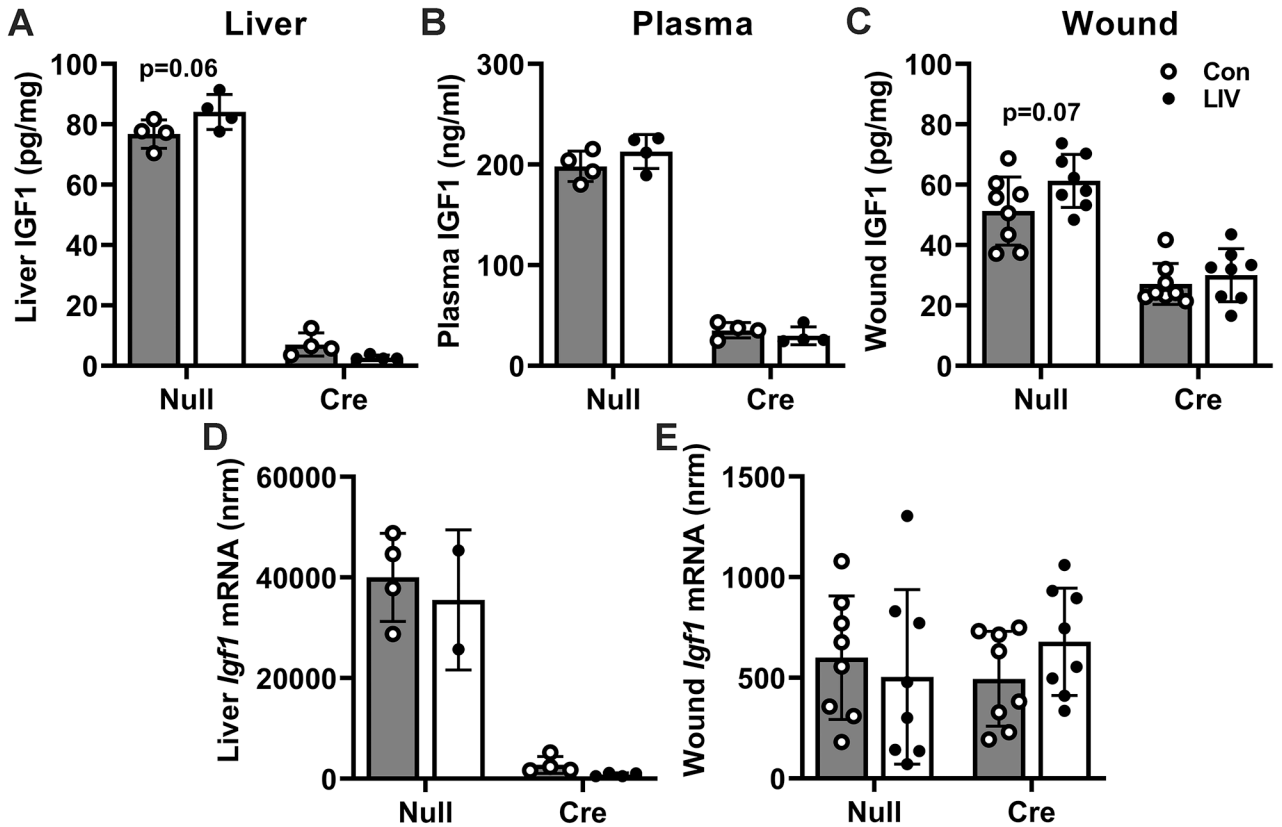


**Figure 3. LIV-induced increase in wound IGF1 levels is absent with liver IGF1 knockdown in HFD-fed mice.**

Liver-specific knockdown of IGF1 induced by administering AAV8.TBGp.Cre (AAV-Cre) to *Igf1* fl/fl mice fed HFD for 16 weeks; controls injected with empty AAV8.pTBG.Null (AAV-Null). After excisional wounding, mice received whole-body LIV or sham control treatment (Con) for 30 min per day. IGF1 levels assessed on day 6 post-injury. (A–C) Liver, peripheral blood plasma, and wound IGF1 protein levels assessed by ELISA. (D,E) Liver and wound *Igf1* mRNA levels assessed by RT-qPCR. *Igf1* mRNA copy numbers normalized (nrm) to those of *Gapdh* and *Rpl4* reference transcripts. For each protein data set, two-way ANOVA showed significant main effects of AAV-cre treatment; wound IGF1 protein also showed main effect of LIV and liver IGF1 protein showed interaction effect. For wound mRNA data, two-way ANOVA showed no significant effects of either AAV-cre or LIV treatment. For liver mRNA data, two-way ANOVA showed a significant main effect of AAV-cre treatment;  $P < 0.05$ . In Šidák's multiple comparisons test, both wound and liver IGF1 protein showed trends ( $0.05 > P > 0.10$ ) of LIV-induced increase in AAV-Null treated mice but not in AAV-Cre treated mice. Mean  $\pm$  SD. For wounds,  $n = 2$  wounds from each of 4 mice per assay. For plasma and liver,  $n = 4$  mice per assay

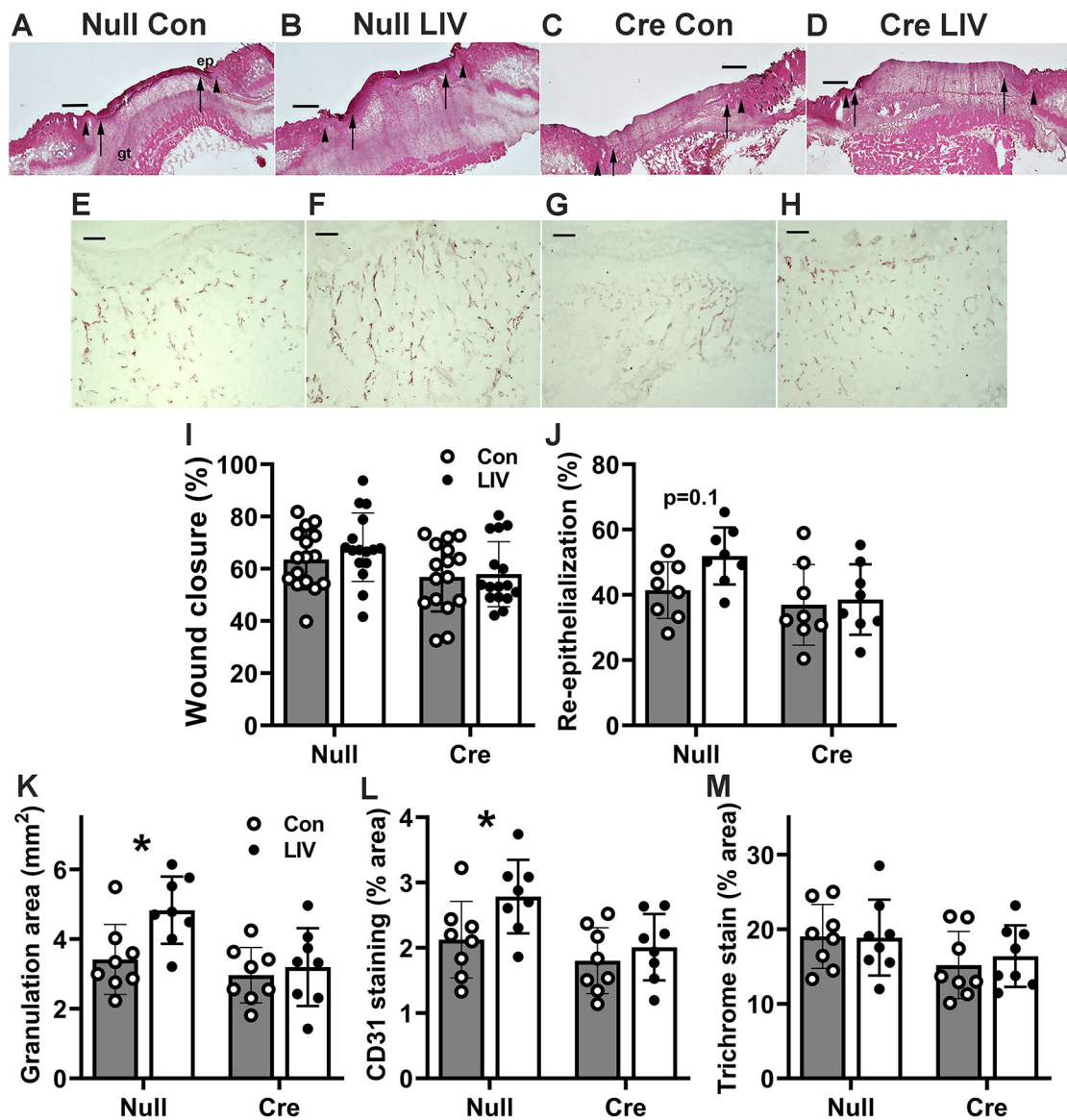


**Figure 4. LIV-induced improvement in wound healing is blocked by liver IGF1 knockdown in HFD-fed mice.**

Liver-specific knockdown of IGF1 induced by administering AAV8.TBGp.Cre (AAV-Cre) to *Igf1* fl/fl mice fed HFD for 16 weeks; controls injected with empty AAV8.pTBG.Null (AAV-Null). After excisional wounding, mice received whole-body LIV or sham control treatment (Con) for 30 min per day. (A–D) Representative images of H&E stained cryosections of center of day 6 wounds from each group of mice. ep: epithelium, gt: granulation tissue. Arrowheads indicate wound edges and arrows indicate tips of epithelial tongues migrating into wound. Scale bar, 0.5 mm. (E–H) Representative images of CD31 stained cryosections of the center of day 6 wounds from each group of mice. gt: granulation tissue. Scale bar, 100  $\mu$ m. (I) Wound closure assessed in digital images of wound surface, expressed as % closure from original wound area. (J) Re-epithelialization assessed in cryosections of wound center, expressed as % closure from wound edges in section. (K) Granulation tissue area assessed in cryosections of wound center. (L) Angiogenesis assessed in cryosections of the

wound center, expressed as % area stained for CD31. (M) Collagen deposition assessed in Trichrome stained cryosections of the wound center, expressed as % area stained blue. For wound closure, two-way ANOVA showed significant main effects of both LIV and AAV-cre treatment; re-epithelialization only showed main effect of AAV-cre treatment. For granulation tissue area and angiogenesis, two-way ANOVA showed significant main effects of both LIV and AAV-cre treatment. \*mean values significantly different between sham-treated and LIV-treated mice in same AAV treatment group by Šidák's multiple comparisons test;  $P < 0.05$ . Wound closure and re-epithelialization also showed trends ( $0.05 < P < 0.10$ ) of LIV-induced increase in AAV-Null treated mice but not in AAV-Cre treated mice in Šidák's multiple comparisons test. Mean  $\pm$  SD. For wound closure,  $n = 4$  wounds from each of 4 mice per group. For all other assays,  $n = 2$  wounds from each of 4 mice per group.

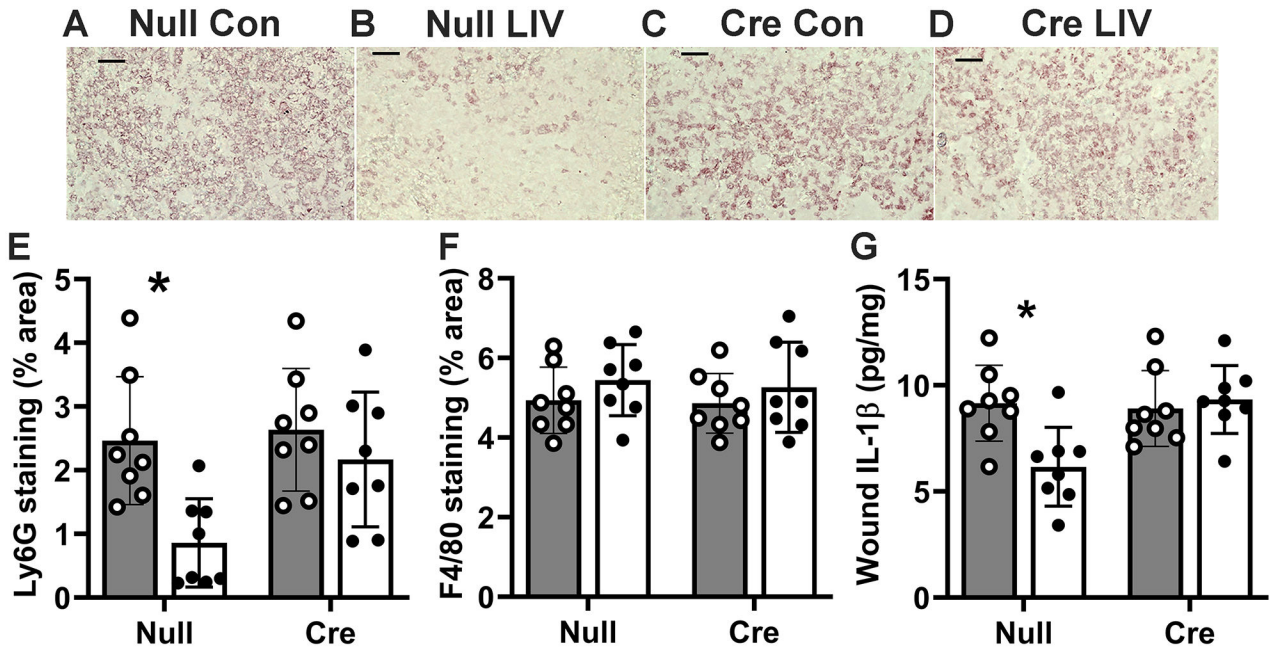


**Figure 5. LIV-induced decrease in wound inflammation is blocked by liver IGF1 knockdown in HFD-fed mice.**

Liver-specific knockdown of IGF1 induced by administering AAV8.TBGp.Cre (AAV-Cre) to *Igf1* fl/fl mice fed HFD for 16 weeks; controls injected with empty AAV8.pTBG.Null (AAV-Null). After excisional wounding, mice received whole-body LIV or sham control treatment (Con) for 30 min per day. (A–D) Representative images of Ly6G stained cryosections of the center of day 6 wounds from each group of mice. Images take from center of wound, close to wound surface. Scale bar, 50  $\mu$ M. (E) Neutrophil accumulation assessed in cryosections of the wound center, expressed as % area stained for Ly6g. (F) Macrophage accumulation assessed in cryosections of the wound center, expressed as % area stained for F4/80. (D) IL-1 $\beta$  protein levels assessed in wound homogenates by ELISA. For neutrophil accumulation and IL-1 $\beta$  protein levels, two-way ANOVA showed significant main effects of both LIV and AAV-Cre treatment; macrophage accumulation showed did not show such effects. \*mean values significantly different between sham-treated and LIV-treated mice in same AAV treatment group by Šidák’s multiple comparisons test;  $P < 0.05$ . For each assay,  $n = 2$  wounds from each of 4 mice.

**Table 1.**

Body weights and blood glucose levels for db/db mice in different experimental groups.

Time point	Con/LIV	Pre-injury Body weight (g)	Post-injury Body weight (g)	Blood glucose (mg/dl)
3 d	Con	48.6 (2.4)	46.1 (2.4)	548 (63)
3 d	LIV	50.2 (2.5)	48.0 (3.2)	567 (29)
6 d	Con	48.7 (1.6)	47.2 (2.6)	582 (25)
6 d	LIV	49.1 (2.6)	46.9 (2.9)	595 (11)
10 d	Con	47.5 (2.2)	45.5 (2.3)	590 (20)
10 d	LIV	48.3 (2.7)	46.7 (2.5)	550 (53)

Values shown are mean (SD)

Author Manuscript

Author Manuscript

Author Manuscript

Author Manuscript

**Table 2.**

Body weights and blood glucose levels for HFD mice in different experimental groups

AAV	LIV	Body weight (g)			Blood glucose (mg/dl)			Insulin (ng/ml)	Growth hormone (ng/ml)
		Pre-AAV	Pre-injury	Post-injury	Pre-AAV	Pre-injury	Post-injury	Post-injury	Post-injury
Null	Con	37.9 (6.1)	36.9 (5.4)	30.1 (4.2)	247 (45)	226 (53)	146 (15)	232 (71)	3.8 (2.0)
Null	LIV	40.1 (5.3)	39.1 (6.2)	32.0 (4.9)	232 (23)	174 (15)	195 (67)	174 (72)	6.7 (3.8)
Cre	Con	38.2 (5.8)	36.4 (5.9)	30.8 (5.6)	243 (29)	176 (30)	161 (14)	377 (201)	65.3 (50.0)*
Cre	LIV	34.5 (5.4)	32.3 (5.3)	26.9 (4.9)	199 (24)	192 (29)	161 (17)	235 (160)	71.2 (35.3)*

Values shown are mean (SD).

\* significantly different from Null Con (p &lt; 0.05).

Author Manuscript

Author Manuscript

Author Manuscript

Author Manuscript